Aerospace Science and Technology 93 (2019) 105299

Contents lists available at ScienceDirect

Aerospace Science and Technology

www.elsevier.com/locate/aescte

Nonlinear control of unmanned aerial vehicles with cable suspended payloads

Ameya R. Godbole, Kamesh Subbarao *

Box 19023, 211 Woolf Hall, Department of Mechanical and Aerospace Engineering, The University of Texas at Arlington, Arlington, United States of America

ARTICLE INFO

Article history:
Received 8 November 2018
Received in revised form 15 April 2019
Accepted 15 July 2019
Available online 17 July 2019

Keywords:
Multi-copter
Extended state observer
Active disturbance rejection control

ABSTRACT

This paper focuses on the mathematical modeling and control of an unmanned aerial system (UAS) with a payload suspended using a cable. The motion of the payload induces disturbances on the aerial platform and needs to be mitigated for stable operation. The solution to this control problem is presented through the implementation of a passivity based controller, and an extended state observer based active disturbance rejection controller. The implementation of the passivity based controller requires the knowledge of higher time derivatives of the payload oscillations. Assuming only the swing angles of the payload with respect to a UAS are measured, these states (primarily the angular velocity) are estimated using a continuous-discrete Kalman Filter. Alternately since, the payload cable swing angle is difficult to measure, an active disturbance rejection controller is designed and implemented wherein the disturbance induced in the system due to the motion of the payload is estimated using the extended state observer. A comparison between the passivity based controller and the extended state observer based active disturbance rejection controller is performed using a high fidelity numerical simulation.

1. Introduction

The problem involving unmanned aerial vehicles for transporting cable suspended payloads has been studied extensively in recent years. Recent advancements in sensor technology and increase in the computation power has led to the availability of inexpensive aerial robots capable of performing aggressive maneuvers and dynamic trajectory generation and tracking. This has opened up the possibility of deploying aerial vehicles to supply aid in disaster situations like floods and earthquakes. The cable suspended approach is an alternative solution to the problem of transporting payload instead of using robotic grippers attached to the aerial vehicles [1]. The primary advantages of using cable suspended payloads is reduced inertia, when compared to the use of robotic grippers while still being able to lift and transport the payload [2], thus providing better response to the change in attitude.

The problem of stabilizing the swinging payload attached to an underactuated system has been solved using feedback linearization [3], Interconnection and Damping Assignment Passivity Based Control [4], [5] and nested saturation [6]. Functionally, it is similar to the problem of stabilizing a payload attached to an overhead crane or an inverted pendulum with horizontal and vertical motion [7]. The problem of trajectory generation for swing-free maneuvers for quadcopters with cable suspended payloads was solved using the dynamic programming approach in [8]. In [9], a downward-facing camera was employed to estimate the state of the payload relative to the quadcopter using an onboard computer and a closed-loop payload control in the full three-dimensional workspace was demonstrated. In [9] the position, velocity, and the yaw angle of the quadcopter are obtained from a VICON system and fused with the payload attitude, and IMU. Additionally, while the paper solves the full problem, it is under the assumption that the cable always remains taut. The motion planning of the load is hence carried out so as to guarantee this condition by synthesizing a load trajectory (differentiable upto 6th order) by solving a quadratic programming problem. The purpose of [9] is to develop a controller that will utilize payload swings and the anticipation of their swings with the rationale that, doing so is more energy optimal (this and the full implication of the payload swings on optimality has not been shown though). In [9], since the intent is to utilize the payload swing for a purpose, it is necessary to estimate the payload motion, and synthesize a load trajectory that will accomplish the stated objectives. In the present paper, we are primarily interested in stabilizing the quadcopter+payload motion in hover, and also during transport of the payload, especially when the quadcopter comes to a rest after approaching a drop location.

* Corresponding author.
E-mail addresses: ameya.godbole@mavs.uta.edu (A.R. Godbole), subbarao@uta.edu (K. Subbarao).

https://doi.org/10.1016/j.ast.2019.07.032
1270-9638/

References [10] and [11] also study the control of the quadcopter and 3-D payload motion, but it is assumed that the payload trajectory is synthesized using a VICON system and subsequently utilized in the control law. In the present work, while the motion of the quadcopter and the payload is restricted to the longitudinal plane, we assume minimal information available for the implementation in the passivity based control framework (motivated by [12] and [4]). Since the controller implementation depends upon the knowledge of the payload swing angle and its derivatives, a state estimator is utilized to estimate the angular velocity of the payload assuming that the payload swing angle is measured.

Since typically, the swing angle of the payload cable is difficult to measure or requires additional sensors to estimate the state of the payload relative to the quadcopter [9], an extended state observer based active disturbance rejection control strategy motivated by [13] is proposed in this work. The payload motion is treated as a disturbance, and an extended state observer [14] is employed to estimate the disturbances introduced in the system due to the motion of the payload. Using these disturbance estimates, a disturbance rejection controller is designed. The extended state observer based active disturbance rejection control strategy relies only on the quadcopter state measurements (longitudinal position, altitude, and attitude). Hence, additional sensors are not required to estimate the state of the payload. A desired control thrust for position tracking is derived first which leads to the synthesis of a desired pitch attitude. A nonlinear control law is designed to track the desired pitch angle to complete the control design.

The paper is organized as follows. Section 2 summarizes the complete mathematical model for a quadcopter with a cable suspended payload. Section 3 presents the design methodology for the passivity based controller and an extended state observer based active disturbance rejection controller to control the position of the quadcopter. Finally, section 4 demonstrates the effectiveness of the control law in numerical simulation using representative scenarios.

2. Governing equations of motion for the quadcopter+payload

The following assumptions are made for the dynamic analysis of the quadcopter with a payload attached to it by a cable.

- The cable is massless and has no slack.
- The payload is approximated as a point mass.
- Aerodynamic effects acting on the payload and the quadcopter are neglected.
- The suspension point is the same as the center of mass of the quadcopter.
- The suspension is frictionless.

Fig. 1 describes the kinematic relations of the quadcopter with a cable attached payload. Consider an inertial coordinate frame {**I**} and a body fixed frame {**B**}, attached to the center of mass of the quadcopter. The generalized coordinates $\boldsymbol{q}$ and the generalized velocities $\dot{\boldsymbol{q}}$ are given by, $\boldsymbol{q} = \begin{bmatrix} x_Q & y_Q & z_Q & \theta_l & \phi_l & \phi & \theta & \psi \end{bmatrix}^T$ and $\dot{\boldsymbol{q}} = \begin{bmatrix} \dot{x}_Q & \dot{y}_Q & \dot{z}_Q & \dot{\theta}_l & \dot{\phi}_l & \dot{\phi} & \dot{\theta} & \dot{\psi} \end{bmatrix}^T$ respectively.

Let $\boldsymbol{X_Q} = \begin{bmatrix} x_Q & y_Q & z_Q \end{bmatrix}^T$ denote the position of the quadcopter in the inertial frame; $[\phi \ \theta \ \psi]^T$ denote the Euler angles (roll, pitch, and yaw); $[\theta_l \ \phi_l]^T$ denotes the swing angle of the cable; m_Q is the mass of the quadcopter; m_l is the mass of the payload; l is the length of the cable.

The position of the center of mass of the payload $\boldsymbol{X_l} = [x_l \ y_l \ z_l]^T$ can be expressed in the inertial frame using the position of the center of mass of the quadcopter in the inertial frame, the payload cable swing angles and the length of the payload cable as

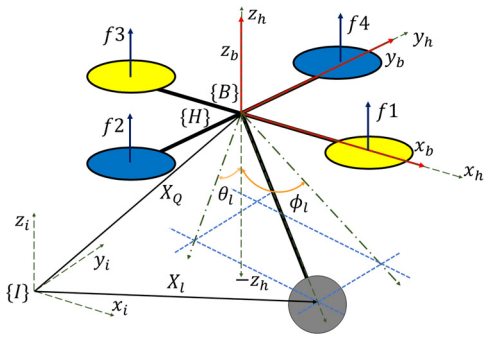

Fig. 1. Description of coordinate frames associated with the quadcopter.

$$\boldsymbol{X_l} = \begin{bmatrix} x_Q & y_Q & z_Q \end{bmatrix}^T + \boldsymbol{R}_y(\phi_l)\,\boldsymbol{R}_x(\theta_l) \begin{bmatrix} 0 & 0 & -l \end{bmatrix}^T, \tag{1}$$

where $\boldsymbol{R}_x(\theta_l)$ and $\boldsymbol{R}_y(\phi_l)$ are the rotation matrices defined as

$$\boldsymbol{R}_y(\phi_l) = \begin{bmatrix} \cos(\phi_l) & 0 & \sin(\phi_l) \\ 0 & 1 & 0 \\ -\sin(\phi_l) & 0 & \cos(\phi_l) \end{bmatrix} \quad \text{and}$$

$$\boldsymbol{R}_x(\theta_l) = \begin{bmatrix} 1 & 0 & 0 \\ 0 & \cos(\theta_l) & -\sin(\theta_l) \\ 0 & \sin(\theta_l) & \cos(\theta_l) \end{bmatrix}$$

Using equation (1), the coordinates of the center of mass of the payload can be expressed in terms of the quadcopter position and the swing angle of the cable as,

$$\begin{aligned} x_l &= x_Q - l\cos(\theta_l)\sin(\phi_l), \\ y_l &= y_Q + l\sin(\theta_l), \\ z_l &= z_Q - l\cos(\theta_l)\cos(\phi_l) \end{aligned} \tag{2}$$

Using equation (2), the velocity kinematics for the payload is given as

$$\dot{\boldsymbol{X}}_l = \boldsymbol{J}_1(\theta_l, \phi_l) \begin{bmatrix} \dot{x}_Q & \dot{y}_Q & \dot{z}_Q & \dot{\theta}_l & \dot{\phi}_l \end{bmatrix}^T \tag{3}$$

where $\boldsymbol{J}_1 \in \mathbb{R}^{3\times 5}$ can be written as

$$\begin{aligned} \boldsymbol{J}_1 &= \begin{bmatrix} 1 & 0 & 0 & l\sin(\phi_l)\sin(\theta_l) & -l\cos(\theta_l)\cos(\phi_l) \\ 0 & 1 & 0 & l\cos(\theta_l) & 0 \\ 0 & 0 & 1 & l\cos(\phi_l)\sin(\theta_l) & l\cos(\theta_l)\sin(\phi_l) \end{bmatrix} \\ &= [\boldsymbol{J}_{11} \mid \boldsymbol{J}_{12}] \end{aligned} \tag{4}$$

where

$$\boldsymbol{J}_{11} = \boldsymbol{I}_{3\times 3} \tag{5}$$

and

$$\boldsymbol{J}_{12} = \begin{bmatrix} l\sin(\phi_l)\sin(\theta_l) & -l\cos(\theta_l)\cos(\phi_l) \\ l\cos(\theta_l) & 0 \\ l\cos(\phi_l)\sin(\theta_l) & l\cos(\theta_l)\sin(\phi_l) \end{bmatrix} \tag{6}$$

The body angular velocity of the quadcopter, $\boldsymbol{\omega} = \begin{bmatrix} \omega_x, \omega_y, \omega_z \end{bmatrix}^T$ is related to the rate of change of Euler angles as

$$\begin{bmatrix} \omega_x \\ \omega_y \\ \omega_z \end{bmatrix} = \begin{bmatrix} 1 & 0 & -\sin(\theta) \\ 0 & \cos(\phi) & \cos(\theta)\sin(\phi) \\ 0 & -\sin(\phi) & \cos(\theta)\cos(\phi) \end{bmatrix} \begin{bmatrix} \dot{\phi} \\ \dot{\theta} \\ \dot{\psi} \end{bmatrix}. \tag{7}$$

and we denote,

$$\boldsymbol{J}_2 = \begin{bmatrix} 1 & 0 & -\sin(\theta) \\ 0 & \cos(\phi) & \cos(\theta)\sin(\phi) \\ 0 & -\sin(\phi) & \cos(\theta)\cos(\phi) \end{bmatrix}. \tag{8}$$

This relation is used in the derivation of the equations of motion of the quadcopter with cable suspended load using the Lagrange-Euler formulation [15,16].

The total kinetic energy of the quadcopter with a cable suspended load can be partitioned as sum of the quadcopter kinetic energy (T_Q),

$$T_Q = \frac{1}{2}m_Q \dot{x_Q}^2 + \frac{1}{2}m_Q \dot{y_Q}^2 + \frac{1}{2}m_Q \dot{z_Q}^2 + \frac{1}{2}\boldsymbol{\omega}^T \boldsymbol{I}_Q \boldsymbol{\omega}$$

and the kinetic energy of the cable suspended payload (T_l),

$$T_l = \frac{1}{2}m_l \dot{x_l}^2 + \frac{1}{2}m_l \dot{y_l}^2 + \frac{1}{2}m_l \dot{z_l}^2$$

where $\boldsymbol{I}_Q$ is the inertia matrix of the quadcopter.

Using the Jacobians derived in eq. (4) and (8), the total kinetic energy $T(\boldsymbol{q}, \dot{\boldsymbol{q}})$ can be written in terms of generalized coordinates as

$$T(\boldsymbol{q}, \dot{\boldsymbol{q}}) = \frac{1}{2}\dot{\boldsymbol{q}}^T [\boldsymbol{M}(\boldsymbol{q})] \dot{\boldsymbol{q}} = \frac{1}{2}\dot{\boldsymbol{q}}^T \left[\boldsymbol{J}(\boldsymbol{q})^T \boldsymbol{M} \boldsymbol{J}(\boldsymbol{q})\right] \dot{\boldsymbol{q}} \tag{9}$$

with

$$\boldsymbol{M} = \begin{bmatrix} \boldsymbol{M}_Q & \boldsymbol{0}_{3\times2} & \boldsymbol{0}_{3\times3} \\ \boldsymbol{0}_{3\times3} & \boldsymbol{M}_l & \boldsymbol{0}_{3\times3} \\ \boldsymbol{0}_{3\times3} & \boldsymbol{0}_{3\times2} & \boldsymbol{I}_Q \end{bmatrix} \tag{10}$$

$$\boldsymbol{J} = \begin{bmatrix} \boldsymbol{I}_{3\times3} & \boldsymbol{0}_{3\times2} & \boldsymbol{0}_{3\times3} \\ \boldsymbol{J}_{11} & \boldsymbol{J}_{12} & \boldsymbol{0}_{3\times3} \\ \boldsymbol{0}_{3\times3} & \boldsymbol{0}_{3\times2} & \boldsymbol{J}_2 \end{bmatrix} \tag{11}$$

and

$$\boldsymbol{M}(\boldsymbol{q}) = \begin{bmatrix} \boldsymbol{M}_Q + \boldsymbol{J}_{11}^T \boldsymbol{M}_l \boldsymbol{J}_{11} & \boldsymbol{J}_{11}^T \boldsymbol{M}_l \boldsymbol{J}_{12} & \boldsymbol{0}_{3\times3} \\ \boldsymbol{J}_{12}^T \boldsymbol{M}_l \boldsymbol{J}_{11} & \boldsymbol{J}_{12}^T \boldsymbol{M}_l \boldsymbol{J}_{12} & \boldsymbol{0}_{3\times3} \\ \boldsymbol{0}_{3\times3} & \boldsymbol{0}_{3\times2} & \boldsymbol{J}_{12}^T \boldsymbol{I}_Q \boldsymbol{J}_{12} \end{bmatrix} \tag{12}$$

where, $\boldsymbol{M}_Q = \text{diag}(m_Q,\ m_Q,\ m_Q)$ and $\boldsymbol{M}_l = \text{diag}(m_l, m_l, m_l)$.

The total potential energy function $V(\boldsymbol{q})$ of the system is the sum of the potential energy of the quadcopter and the payload and is given as

$$V(\boldsymbol{q}) = m_Q g z_Q + m_l g \left(z_Q - l\cos(\theta_l)\cos(\phi_l)\right) \tag{13}$$

where g is the acceleration due to gravity.

Using the expressions for the kinetic and potential energy, the Lagrangian is formulated as

$$\mathcal{L} = T(\boldsymbol{q}, \dot{\boldsymbol{q}}) - V(\boldsymbol{q})$$

Using the Euler-Lagrange formulation, the governing equations for the quadcopter with cable suspended load are compactly represented as

$$\boldsymbol{M}(\boldsymbol{q})\ddot{\boldsymbol{q}} + \boldsymbol{C}(\boldsymbol{q}, \dot{\boldsymbol{q}})\dot{\boldsymbol{q}} + \boldsymbol{G}(\boldsymbol{q}) = \boldsymbol{f}_{ext} + \boldsymbol{d}_{ext} \tag{14}$$

Note, typical disturbances $\boldsymbol{d}_{ext}$ that could be present in the equations of motion could be those due to unmodeled interactions of the payload+cable+quadcopter (due to cable mass), and atmospheric disturbances. This paper doesn't consider these disturbances. Although, it should be mentioned that such bounded disturbances can be accommodated using appropriate robustifying terms in the control design. Also, $\boldsymbol{f}_{ext} = \begin{bmatrix} F_x & F_y & F_z & 0 & 0 & \tau_x & \tau_y & \tau_z \end{bmatrix}^T$ denotes the control input to the quadcopter in the inertial frame. It is easily seen that

$$\begin{bmatrix} F_x \\ F_y \\ F_z \end{bmatrix} = \boldsymbol{R}(\phi, \theta, \psi) \begin{bmatrix} 0 \\ 0 \\ u_1 \end{bmatrix} \tag{15}$$

where, $\boldsymbol{R}(\phi, \theta, \psi)$ is the rotation matrix translating the force inputs from the quadcopter body frame $\{\boldsymbol{B}\}$ to the inertial frame $\{\mathbf{I}\}$.

In terms of the individual thrust forces produced by the quadcopter (f_1, f_2, f_3 and f_4), the control inputs are determined as

$$u_1 = f_1 + f_1 + f_3 + f_4 \tag{16}$$

$$\tau_x = L(f_4 - f_2) \tag{17}$$

$$\tau_y = L(f_3 - f_1) \tag{18}$$

$$\tau_z = -Q_1 + Q_2 - Q_3 + Q_4 \tag{19}$$

where Q_1, Q_2, Q_3, Q_4 are the moments generated by each of the rotors and L is the arm length of the quadcopter.

3. Solution methodology (controller design)

Consider the translational dynamics of the quadcopter given in equation (14). In general,

$$\begin{aligned} \ddot{x}_Q &= f_x\left(m_Q, m_l, l, \theta_l, \phi_l, \dot{\theta}_l, \dot{\phi}_l, \ddot{\theta}_l, \ddot{\phi}_l\right) + F_x \\ \ddot{y}_Q &= f_y\left(m_Q, m_l, l, \theta_l, \phi_l, \dot{\theta}_l, \dot{\phi}_l, \ddot{\theta}_l, \ddot{\phi}_l\right) + F_y \\ \ddot{z}_Q &= f_z\left(m_Q, m_l, l, g, \theta_l, \phi_l, \dot{\theta}_l, \dot{\phi}_l, \ddot{\theta}_l, \ddot{\phi}_l\right) + F_z \end{aligned} \tag{20}$$

In general, it is true that if the payload is disturbed arbitrarily, the payload has both longitudinal swing and lateral motion. In this paper, we assume the perturbations are only in the longitudinal swing. Note, pure longitudinal swing doesn't affect the system motion in the lateral direction, unless there is asymmetry in the quadcopter and/or the payload attachment, or if there are external wind disturbances. Similarly, in pure longitudinal motion, if the quadcopter only moves in the x_i–z_i plane, and comes to a stop or accelerates, the payload motion is only in the longitudinal swing. Hence, the longitudinal plane restriction of the quadcopter with cable suspended payload in x_i–z_i inertial plane is considered to design a control solution when the motion of the payload cable is purely in the longitudinal plane. The simplified model can be obtained by applying constraints on the dynamic model obtained in equation (14). Then, the system dynamics for the quadcopter with cable suspended load in the x_i–z_i plane is given by

$$\left(m_Q + m_l\right)(\ddot{z}_Q + g) + m_l l\left(\cos(\phi_l)\dot{\phi}_l^2 - \sin(\phi_l)\ddot{\phi}_l\right) = F_z \tag{21}$$

$$\left(m_Q + m_l\right)\ddot{x}_Q + m_l l\left(\sin(\phi_l)\dot{\phi}_l^2 + \cos(\phi_l)\ddot{\phi}_l\right) = F_x \tag{22}$$

$$m_l l^2 \ddot{\phi}_l + m_l l \sin(\phi_l)\ddot{z}_Q - m_l l\cos(\phi_l)\ddot{x}_Q + m_l g l \sin(\phi_l) = 0 \tag{23}$$

$$I_{yy}\dot{\omega}_y = \tau_y \tag{24}$$

where

$$\begin{aligned} F_x &= u_1 \sin(\theta), \\ F_z &= u_1 \cos(\theta), \end{aligned} \tag{25}$$

are the control inputs.

Given the combined dynamics of the quadcopter and the cable suspended payload, control functions f_i are sought such that ϕ_l, and $\dot{\phi}_l \to 0$ as $t \to \infty$ for any initial condition errors and bounded disturbances. Two approaches are used to solve this problem, and the results obtained from each compared,

- Passivity Based Controller
- Extended State Observer based Active Disturbance Rejection Controller

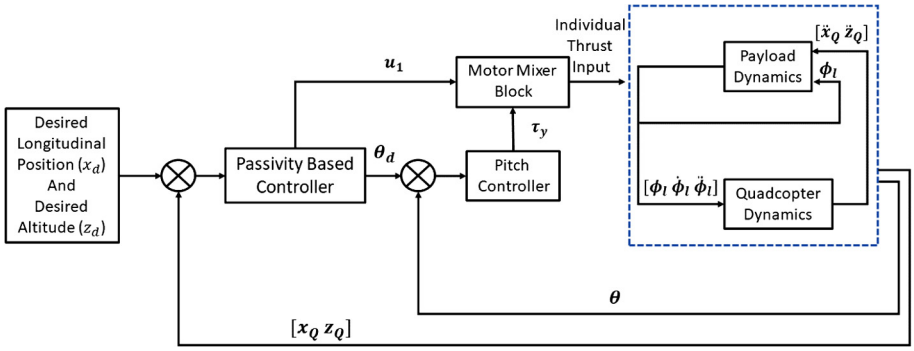

Fig. 2. Control architecture of the quadcopter with cable suspended payload using passivity based controller.

3.1. Passivity Based Controller (PBC)

In this paper, we adopt a similar control strategy as in [12, 15] i.e. design a passivity based controller to stabilize the system by controlling the overall energy of the system. Fig. 2 shows the control architecture of the quadcopter with cable suspended payload in x_i–z_i plane using passivity based controller. The system is decoupled into an inner control loop to stabilize the attitude dynamics of the quadcopter and an outer loop to stabilize the translational dynamics of the quadcopter along with the pendulum dynamics [6]. The outer loop is further decoupled to stabilize the altitude of the quadcopter (z_Q), longitudinal position of the quadcopter (x_Q) and the swing of the pendulum.

From equations (21) and (22)

$$\ddot{z}_Q = \frac{u_1 \cos(\theta)}{m_Q + m_l} - g - \frac{m_l l}{m_Q + m_l}\left[\cos(\phi_l)\,\dot{\phi}_l^2 + \sin(\phi_l)\,\ddot{\phi}_l\right] \tag{26}$$

$$\ddot{x}_Q = \frac{u_1 \sin(\theta)}{m_Q + m_l} - \frac{m_l l}{m_Q + m_l}\left[\sin(\phi_l)\,\dot{\phi}_l^2 - \cos(\phi_l)\,\ddot{\phi}_l\right] \tag{27}$$

Using equations (23), (26), and (27),

$$\ddot{\phi}_l = \frac{-\sin(\phi_l - \theta)\,u_1}{m_Q l} \tag{28}$$

Substituting equation (28) in equations (26) and (27),

$$\ddot{z}_Q = \frac{1}{m_Q + m_l}\left[\cos(\theta) + \frac{m_l}{2m_Q}\left(\cos(\theta) - \cos(\theta - 2\phi_l)\right)\right]u_1 - g - \frac{m_l l \cos(\phi_l)\,\dot{\phi}_l^2}{m_Q + m_l} \tag{29}$$

$$\ddot{x}_Q = -\frac{m_l l \sin(\phi_l)\,\dot{\phi}_l^2}{m_Q + m_l} + \frac{1}{m_Q + m_l} \times \left[\sin(\theta) + \frac{m_l}{2m_Q}\left(\sin(\theta) - \sin(\theta - 2\phi_l)\right)\right]u_1 \tag{30}$$

For hover conditions and small pitch angles of the quadcopter, the attitude dynamics can be approximated using $\cos(\theta) \approx 1$ and $\sin(\theta) \approx \theta$ and treating θ as the control input θ_d results into following dynamics for $\ddot{x}_Q$ and $\ddot{z}_Q$

$$\ddot{z}_Q = \frac{1}{m_Q + m_l}\left[1 + \frac{m_l}{2m_Q}\left(1 - \cos(2\phi_l) - \theta_d \sin(2\phi_l)\right)\right]u_1 - g - \frac{m_l l \cos(\phi_l)\,\dot{\phi}_l^2}{m_Q + m_l} \tag{31}$$

$$\ddot{x}_Q = -\frac{m_l l \sin(\phi_l)\,\dot{\phi}_l^2}{m_Q + m_l} + \frac{g\theta_d}{m_Q + m_l} + \frac{1}{m_Q + m_l} \times \left[\frac{m_l}{2m_Q}\left(\theta_d - \theta_d \cos(2\phi_l) - \sin(2\phi_l)\right)\right]u_1 \tag{32}$$

Near hovering condition, $u_1 \approx (m_Q + m_l)\,g$ and longitudinal dynamics can only be controlled by θ_d. This results into the following for $\ddot{x}_Q$,

$$\ddot{x}_Q = \theta_d\left[g + \frac{g m_l}{2m_Q}\left(1 - \cos(2\phi_l)\right)\right] - \frac{m_l l \sin(\phi_l)\,\dot{\phi}_l^2}{m_l + m_Q} - \frac{m_l g \sin(2\phi_l)}{2m_Q} \tag{33}$$

Thus, choosing the control inputs θ_d and u_1 as

$$\theta_d = \frac{u_x + \frac{m_l l \sin(\phi_l)\dot{\phi}_l^2}{m_l + m_Q} + \frac{m_l g \sin(2\phi_l)}{2m_Q}}{\left[g + \frac{g m_l}{2m_Q}\left(1 - \cos(2\phi_l)\right)\right]} \tag{34}$$

$$u_1 = \frac{(m_Q + m_l)\left(g + \frac{m_l l \cos(\phi_l)\dot{\phi}_l^2}{m_Q + m_l} + u_z\right)}{\left[1 + \frac{m_l}{2m_Q}\left(1 - \cos(2\phi_l) - \theta_d \sin(2\phi_l)\right)\right]} \tag{35}$$

and with

$$u_z = -k_p^z(z_Q - z_d) - k_d^z\left(\dot{z}_Q - \dot{z}_d\right) + \ddot{z}_d$$
$$u_x = -k_p^x(x_Q - z_d) - k_d^x\left(\dot{x}_Q - \dot{x}_d\right) + \ddot{x}_d$$

the closed loop position tracking dynamics of the quadcopter are reduced to,

$$\ddot{z}_Q = -k_p^z(z_Q - z_d) - k_d^z\left(\dot{z}_Q - \dot{z}_d\right) + \ddot{z}_d$$
$$\ddot{x}_Q = -k_p^x(x_Q - x_d) - k_d^x\left(\dot{x}_Q - \dot{x}_d\right) + \ddot{x}_d$$

which ensures $x_Q \to x_d$ and $z_Q \to z_d$. The rate of decay and other transient characteristics of the tracking errors are controlled by tuning the positive gains k_p^z, k_d^z, k_p^x, and k_d^x. Note, while the control design assumes the quadcopter is in hover, and small angle approximation of the pitch angle is used, the control terms in equations (34) and (35) are nonlinear due to the presence of the trigonometric and quadratic terms involving the payload longitudinal swing angle and its derivative. These nonlinear functions serve as feedback linearizing terms for equations (31) and (33).

Remark. Clearly, the passivity based controller shown in equations (34) and (35) requires higher derivatives of the payload swing angle. The measurement of the swing angle and all its higher order derivatives is a challenging task. Some alternatives to alleviate these difficulties are explored in this section.

Specifically at the hover state, the dynamics of the swinging payload can be assumed to be equivalent to the dynamics of a simple pendulum linearized about ϕ_l at the present instant, is given by

$$\Delta\ddot{\phi}_l \approx -\frac{g}{l}\Delta\phi_l$$

Thus, if the swing angle is measured, then using this approximation, the angular velocity as well as the acceleration of the swinging payload can be estimated. Also, under this assumption all higher order derivatives are successively obtained.

Note, assuming that the angle measurements for the payload swing are available, the angular velocity of the swinging cable can also be estimated using a Continuous-Discrete Kalman Filter (CDKF) driven by the swing angle measurements.

In our specific implementation, the propagation is continuous while the measurement updates happen at discrete instants (every 0.01 s). The CDKF utilizes the simplified one degree-of-freedom dynamics:

$$\Delta\ddot{\phi}_l = -\frac{g}{l}\Delta\phi_l + w_\phi(t)$$

where $w_\phi(t)$ is a zero mean white noise process with covariance 0.25 rad^2/s^4.

The measurement equation is

$$\Delta\tilde{\phi}_l = \Delta\phi_l + v_\phi(t)$$

The measurement error $v_\phi(t)$ is also assumed to be a zero-mean white noise process with variance 0.01 rad^2. Additionally, $w_\phi(t)$, and $v_\phi(t)$ are assumed to be uncorrelated. The derivation of the CDKF is straightforward and can be found in [17].

3.2. Extended State Observer (ESO) based active disturbance rejection controller

The concept of total disturbance, its estimation, and rejection was introduced in [14]. To understand the concept, consider a second-order single input single output (SISO) system

$$\begin{aligned}\dot{y}_1 &= y_2\\ \dot{y}_2 &= f(y_1, y_2, \omega(t), t) + bu\\ y &= y_1\end{aligned} \tag{36}$$

where y is the output which is measured and controlled; u is the control input; $f(y_1, y_2, \omega(t), t)$ is a function of both states and external disturbances $\omega(t)$ which is to be overcome and is denoted as the "total disturbance".

Treating $y_3 = f(y_1, y_2, \omega(t), t)$ as an additional state and $G(t) = \dot{f}(y_1, y_2, \omega(t), t)$, with $G(t)$ unknown, the plant dynamics is re-written as

$$\begin{aligned}\dot{y}_1 &= y_2\\ \dot{y}_2 &= y_3 + bu\\ \dot{y}_3 &= G(t)\\ y &= y_1\end{aligned} \tag{37}$$

The objective here is to control the output y using the control signal u. Here the total disturbance $f(y_1, y_2, \omega(t), t)$ does not need to be known and can be estimated along with the states of the system using an extended state observer with system output $y = y_1$ and control signal u as the input to the observer, which is constructed as follows

$$\begin{aligned}\dot{\hat{y}}_1 &= \hat{y}_2 - \beta_1 s_1\\ \dot{\hat{y}}_2 &= \hat{y}_3 + bu - \beta_2 s_2\\ \dot{\hat{y}}_3 &= -\beta_3 s_3\end{aligned} \tag{38}$$

where β_1, β_2 and β_3 are the observer gains; $\hat{y}_1$, $\hat{y}_2$ and $\hat{y}_3$ are the estimates of y_1, y_2 and $f(y_1, y_2, \omega(t), t)$ respectively; and s_1, s_2, and s_3 are ESO functions that will be determined later.

Lemma 1. *Given that the system modeled by equation (36) is locally observable, the extended state observer in equation (38) for the model in equation (36) ensures that the errors, $\|\hat{y}_i - y_i\| \leq \varepsilon$ are uniformly bounded as $t \to \infty$, where $\varepsilon > 0$.*

Proof. Denote the estimation errors as $e_i = \hat{y}_i - y_i$. The error dynamics is then obtained as

$$\begin{aligned}\dot{e}_1 &= -\beta_1 s_1 + e_2\\ \dot{e}_2 &= -\beta_2 s_2 + e_3\\ \dot{e}_3 &= -\beta_3 s_3 - G(t)\end{aligned} \tag{39}$$

Choosing all $s_i = e_1$, and defining $\boldsymbol{e} = [e_1\ e_2\ e_3]^T$, the above can be re-written as

$$\dot{\boldsymbol{e}} = \boldsymbol{A}\boldsymbol{e} + \boldsymbol{B}G \tag{40}$$

where $\boldsymbol{A} = \begin{bmatrix} -\beta_1 & 1 & 0\\ -\beta_2 & 0 & 1\\ -\beta_3 & 0 & 0\end{bmatrix}$ and $\boldsymbol{B} = \begin{bmatrix} 0\\ 0\\ -1\end{bmatrix}$. For $\beta_1, \beta_2, \beta_3$ all > 0, $\boldsymbol{A}$ is Hurwitz. Thus, if $G(t)$ is bounded, i.e. $\|G(t)\| < \delta$, then the estimation errors, $\boldsymbol{e}(t)$ are also bounded. Choosing a candidate Lyapunov function:

$$V = \frac{1}{2}\boldsymbol{e}^T\boldsymbol{P}\boldsymbol{e} \tag{41}$$

where $\boldsymbol{P} = \boldsymbol{P}^T > 0$ and computing the derivative of V along the dynamics in equation (40) we obtain:

$$\dot{V} = -\frac{1}{2}\boldsymbol{e}^T\boldsymbol{Q}\boldsymbol{e} + \boldsymbol{e}^T\boldsymbol{P}\boldsymbol{B}G \tag{42}$$

where $\boldsymbol{Q} = \boldsymbol{Q}^T > 0$, and $\boldsymbol{P}\boldsymbol{A} + \boldsymbol{A}^T\boldsymbol{P} = -\boldsymbol{Q}$. The solution to this Lyapunov equation i.e. $\boldsymbol{P}$ for a chosen $\boldsymbol{Q}$ is guaranteed since $\boldsymbol{A}$ is Hurwitz. We can further show that,

$$\dot{V} \leq -\frac{1}{2}\boldsymbol{e}^T(\boldsymbol{Q} - \alpha\boldsymbol{I})\boldsymbol{e} + \frac{1}{2\alpha}G^T\boldsymbol{B}^T\boldsymbol{P}^2\boldsymbol{B}G \tag{43}$$

Thus,

$$\begin{aligned}\dot{V} &\leq -\frac{1}{2}\boldsymbol{e}^T(\boldsymbol{Q} - \alpha\boldsymbol{I})\boldsymbol{e} + \frac{1}{2\alpha}\|\boldsymbol{B}^T\boldsymbol{P}^2\boldsymbol{B}\|\delta^2\\ &\leq -\frac{1}{2}\boldsymbol{e}^T(\boldsymbol{Q} - \alpha\boldsymbol{I})\boldsymbol{e} + \frac{\lambda_{\max}^2(\boldsymbol{P})}{2\alpha}\delta^2\\ &\leq -\left(\frac{\lambda_{\min}(\boldsymbol{Q} - \alpha\boldsymbol{I})}{\lambda_{\max}(\boldsymbol{P})}\right)V + \frac{\lambda_{\max}^2(\boldsymbol{P})}{2\alpha}\delta^2\end{aligned} \tag{44}$$

where $\lambda_{\min}(\cdot)$ and $\lambda_{\max}(\cdot)$ are the minimum and maximum eigenvalues of $(\cdot)$ respectively. Clearly, the errors converge as per equation (44) to a residual set given by equation (44). □

Thus, using the estimate of the total disturbance $\hat{y}_3$ for compensation and choosing u as

$$u = \frac{u_0 - \hat{y}_3}{b}$$

with

$$u_0 = -k_p(y_1 - y_{1d}) - k_d(\dot{y}_1 - \dot{y}_{1d}) + \ddot{y}_{1d}$$

where $k_p > 0$ and $k_d > 0$ are the controller gains, and y_{1d} being the desired value for the state y_1. This reduces the plant dynamics to

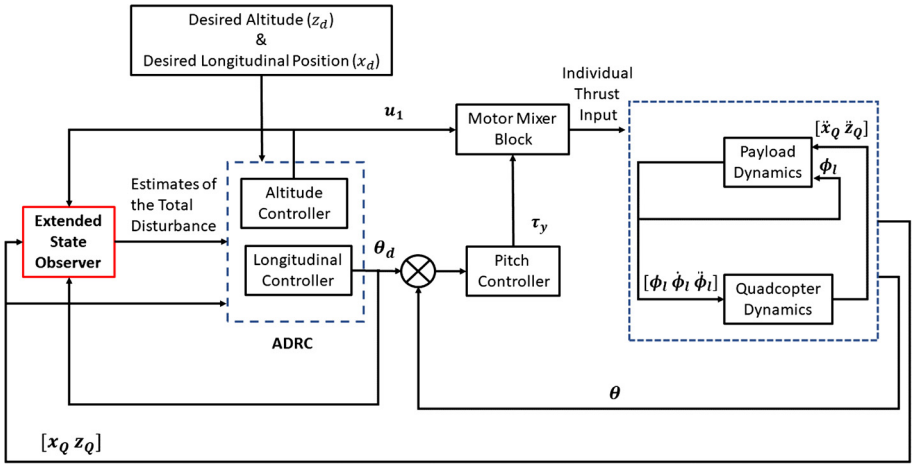

Fig. 3. Control architecture of the quadcopter with cable suspended payload using extended state observer based active disturbance rejection controller.

$$\dot{y}_1 = y_2$$
$$\dot{y}_2 = -k_p\,(y_1 - y_{1d}) - k_d\,(\dot{y}_1 - \dot{y}_{1d}) + \ddot{y}_{1d} - e_3$$
$$y = y_1 \tag{45}$$

which ensures $\|y_1 - y_{1d}\|$ is bounded (Note, e_3 is bounded as shown previously). This transforms the control problem to that of estimation and disturbance rejection.

Fig. 3 gives the control architecture of the quadcopter with cable suspended payload using the extended state observer based active disturbance rejection controller. The system is decoupled into an inner control loop to stabilize the attitude dynamics of the quadcopter and an outer loop to stabilize the translational dynamics of the quadcopter along with the pendulum dynamics. The outer loop is further decoupled to stabilize the altitude of the quadcopter (z_Q), longitudinal position of the quadcopter (x_Q) and the swing of the pendulum using an active disturbance rejection controller. An extended state observer is constructed to estimate the disturbance in the altitude dynamics and the longitudinal dynamics of the quadcopter with cable suspended payload. The input to the extended state observer includes the altitude of the quadcopter (z_Q), the longitudinal position of the quadcopter (x_Q) and the control inputs to the quadcopter. The extended state observer estimates the disturbances which are used by the active disturbance rejection controller to control the altitude and the longitudinal position of the quadcopter. The active disturbance rejection controller is further decoupled into an altitude controller and a longitudinal position controller, which are discussed in the following sections.

3.2.1. Altitude controller

From equation (21)

$$\ddot{z}_Q = \frac{u_1\cos(\theta)}{m_Q + m_l} - g - \frac{m_l l}{m_Q + m_l}\left[\cos(\phi_l)\,\dot{\phi}_l^2 + \sin(\phi_l)\,\ddot{\phi}_l\right] \tag{46}$$

Near hovering conditions and small pitch angle of the quadcopter, $\cos(\theta) \approx 1$ and $\sin(\theta) \approx \theta$. Using this assumption, eq. (46) can be written as

$$\ddot{z}_Q = \frac{u_1}{m_Q + m_l} + f_z\left(m_Q, m_l, l, g, \phi_l, \dot{\phi}_l, \ddot{\phi}_l\right)$$

where

$$f_z\left(m_Q, m_l, l, g, \phi_l, \dot{\phi}_l, \ddot{\phi}_l\right) = -g - \frac{m_l l}{m_Q + m_l}\left[\cos(\phi_l)\,\dot{\phi}_l^2 + \sin(\phi_l)\,\ddot{\phi}_l\right]$$

is the total disturbance associated with the altitude dynamics.

Let $z_1 = z_Q$, $z_2 = \dot{z}_Q$ and treating $z_3 = f_z(m_Q, m_l, l, g, \phi_l, \dot{\phi}_l, \ddot{\phi}_l)$ as an additional state, the state equations for the altitude dynamics can be written as,

$$\dot{z}_1 = z_2$$
$$\dot{z}_2 = \frac{u_1}{m_Q + m_l} + z_3$$
$$\dot{z}_3 = G_z(t)$$
$$y_z = z_1$$

where $\dot{z}_3 = G_z(t)$ is the dynamics of the total disturbance which is unknown; y_z is the output which is measured and needs to be controlled.

The extended state observer for the system is now constructed as

$$\dot{\hat{z}}_1 = \hat{z}_2 - \beta_{z1}\left(\hat{z}_1 - y_z\right)$$
$$\dot{\hat{z}}_2 = \hat{z}_3 + bu - \beta_{z2}\left(\hat{z}_1 - y_z\right)$$
$$\dot{\hat{z}}_3 = -\beta_{z3}\left(\hat{z}_1 - y_z\right)$$

where β_{z1}, β_{z2} and β_{z3} are the observer gains; $\hat{z}_1$, $\hat{z}_2$ and $\hat{z}_3$ are the estimates of z_1, z_2 and $f_z\left(m_Q, m_l, l, g, \phi_l, \dot{\phi}_l, \ddot{\phi}_l\right)$ respectively.

Using the estimate of the total disturbance $\hat{z}_3$ for compensation and choosing u_1 as

$$u_1 = \left(u_{z0} - \hat{z}_3\right)\left(m_Q + m_l\right)$$

with

$$u_{z0} = -k_{pz}\,(z_1 - z_{1d}) - k_{dz}\,(\dot{z}_1 - \dot{z}_{1d}) + \ddot{z}_{1d}$$

where k_{pz} and k_{dz} are the controller gains and z_{1d} as the desired values for the state z_1. This reduces the plant dynamics to

$$\dot{z}_1 = z_2$$
$$\dot{z}_2 = -k_{pz}\,(z_1 - z_{1d}) - k_{dz}\,(\dot{z}_1 - \dot{z}_{1d}) + \ddot{z}_{1d} - \Delta z_3$$
$$y_z = z_1$$

where $\Delta z_3 = \hat{z}_3 - z_3$. The above ensures $\|z_1 - z_{1d}\|$ is bounded. The rate of decay and other transient characteristics of the tracking errors are controlled by tuning the positive gains k_{pz} and k_{dz}.

3.2.2. Longitudinal position controller

From equation (22), the longitudinal dynamics of a quadcopter with cable suspended payload restricted in a x_i–z_i inertial plane is given as,

$$\ddot{x}_Q = \frac{u_1 \sin(\theta)}{m_Q + m_l} - \frac{m_l l}{m_Q + m_l}\left[\sin(\phi_l)\,\dot{\phi}_l^2 - \cos(\phi_l)\,\ddot{\phi}_l\right]$$

Near hovering condition, $u_1 \approx (m_Q + m_l)\,g$ and longitudinal dynamics can only be controlled by controlling the pitch angle θ. Treating θ as the control input θ_d which is the desired pitch angle results into the following for $\ddot{x}_Q$,

$$\ddot{x}_Q = g\theta_d + f_x\left(m_Q, m_l, l, \phi_l, \dot{\phi}_l, \ddot{\phi}_l\right)$$

where $f_x\left(m_Q, m_l, l, \phi_l, \dot{\phi}_l, \ddot{\phi}_l\right) = -\frac{m_l l}{m_Q + m_l}\left[\sin(\phi_l)\,\dot{\phi}_l^2 - \cos(\phi_l)\,\ddot{\phi}_l\right]$ is the total disturbance.

Let $x_1 = x_Q$, $x_2 = \dot{x}_Q$ and treating $x_3 = f_x\left(m_Q, m_l, l, \phi_l, \dot{\phi}_l, \ddot{\phi}_l\right)$ as an additional state, the state equations for the longitudinal dynamics can be written as,

$$\dot{x}_1 = x_2$$

$$\dot{x}_2 = g\theta_d + x_3$$

$$\dot{x}_3 = G_x(t)$$

$$y_x = x_1$$

where $\dot{x}_3 = G_x(t)$ is the dynamics of the total disturbance which is unknown; y_x is the output which is measured and needs to be controlled.

The extended state observer for the system is now constructed as

$$\dot{\hat{x}}_1 = \hat{x}_2 - \beta_{x1}\left(\hat{x}_1 - y_x\right)$$

$$\dot{\hat{x}}_2 = \hat{x}_3 + g\theta_d - \beta_{x2}\left(\hat{x}_1 - y_x\right)$$

$$\dot{\hat{x}}_3 = -\beta_{x3}\left(\hat{x}_1 - y_x\right)$$

where β_{x1}, β_{x2} and β_{x3} are the observer gains; $\hat{x}_1$, $\hat{x}_2$ and $\hat{x}_3$ are the estimates of x_1, x_2 and $f_x\left(m_Q, m_l, l, \phi_l, \dot{\phi}_l, \ddot{\phi}_l\right)$ respectively.

Using the estimate of the total disturbance $\hat{x}_3$ for compensation and choosing θ_d as

$$\theta_d = \frac{\theta_{d0} - \hat{x}_3}{g}$$

with

$$\theta_{d0} = -k_{px}\left(x_1 - x_{1d}\right) - k_{dx}\left(\dot{x}_1 - \dot{x}_{1d}\right) + \ddot{x}_{1d}$$

where k_{px} and k_{dx} are the controller gains and x_{1d} as the desired values for the state x_1. This reduces the plant dynamics to

$$\dot{x}_1 = x_2$$

$$\dot{x}_2 = -k_{px}\left(x_1 - x_{1d}\right) - k_{dx}\left(\dot{x}_1 - \dot{x}_{1d}\right) + \ddot{x}_{1d} - \Delta x_3$$

$$y_x = x_1$$

where $\Delta x_3 = \hat{x}_3 - x_3$. The above ensures $\|x_1 - x_{1d}\|$ is bounded. The rate of decay and other transient characteristics of the tracking errors are controlled by tuning the positive gains k_{px} and k_{dx}.

3.3. Pitch controller

The pitch control design procedure can either use θ_d synthesized using the passivity based controller or extended state observer based active disturbance rejection controller. The pitch controller can be designed using the pitch tracking error e_θ, which is defined as

$$e_\theta = \theta - \theta_d$$

and

$$\dot{e}_\theta = \dot{\theta} - \dot{\theta}_d$$

We seek a very tightly controlled pitch loop, so the pitch errors are prescribed to converge to zero exponentially with a decay rate of λ_θ. Thus, the pitch error dynamics takes the form

$$\dot{e}_\theta = -\lambda_\theta e_\theta$$

The desired pitch rate

$$\omega_{yd} = -\lambda_\theta e_\theta + \dot{\theta}_d$$

ensures that $e_\theta \to 0$, as $t \to \infty$.

The pitch rate error (e_ω) is then obtained as

$$e_\omega = \omega_y - \omega_{yd}$$

The pitch rate errors are also prescribed to converge to zero exponentially with a decay rate of λ_ω. Thus, the desired pitch rate error dynamics takes the form

$$\dot{e}_\omega = -\lambda_\omega e_\omega$$

Thus, $\dot{\omega}_y - \dot{\omega}_{yd} = -\lambda_\omega e_\omega$ and the control law for the pitch dynamics is determined as

$$\tau_y = I_{yy}\left(-\lambda_\omega e_\omega + \dot{\omega}_{yd}\right)$$

It is noted that the above procedure is a nested design process as in [18].

4. Simulation results

The model and controller parameters used to demonstrate the efficacy of both the passivity based controller and the extended state observer based active disturbance rejection controller implemented on the quadcopter with a cable suspended payload, in the simulation environment, are tabulated in Appendix A, Tables 1–5. The following cases are used to compare the performance of the controllers

1. Case 1: Quadcopter in Hover Mode and the Payload is Perturbed
2. Case 2: Quadcopter Moving with a Constant Speed along x_i axis is commanded to go in the Hover Mode

The performance of the controllers derived using the longitudinal plane restriction is compared in the simulation environment using the mathematical model of quadcopter+payload with longitudinal plane restriction and the complete nonlinear model of quadcopter+payload.

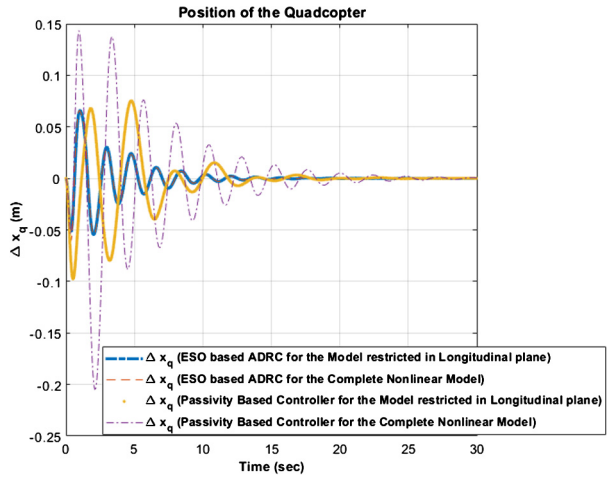

Fig. 4. Longitudinal position of the quadcopter (x_Q).

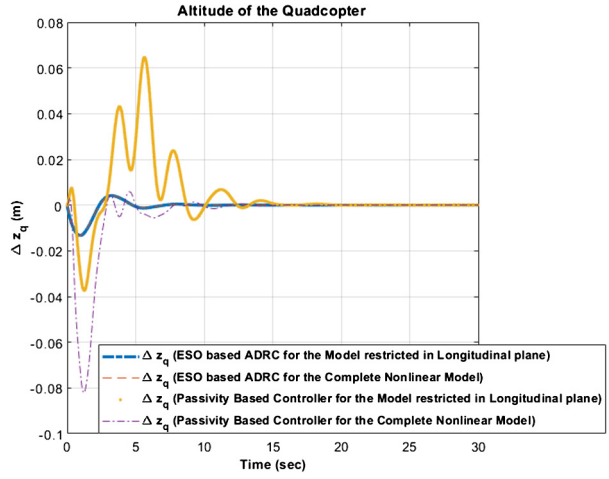

Fig. 5. Altitude of the quadcopter (z_Q).

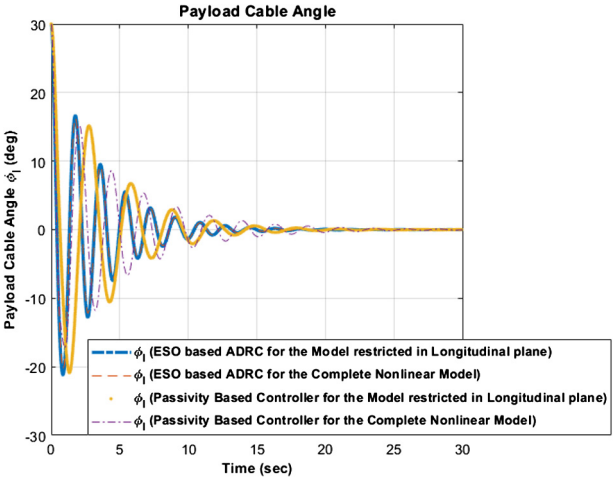

Fig. 6. Payload cable angle history.

4.1. Case 1: Quadcopter in hover mode and the payload is perturbed

The quadcopter is in a hovering state at the start of the simulation. The payload cable angle at the start of the simulation is 30°. Figs. 4, 5, 6 and 7 compares the performance of the passivity based controller and the extended state observer based active disturbance rejection controller. At the start of the simulation, there

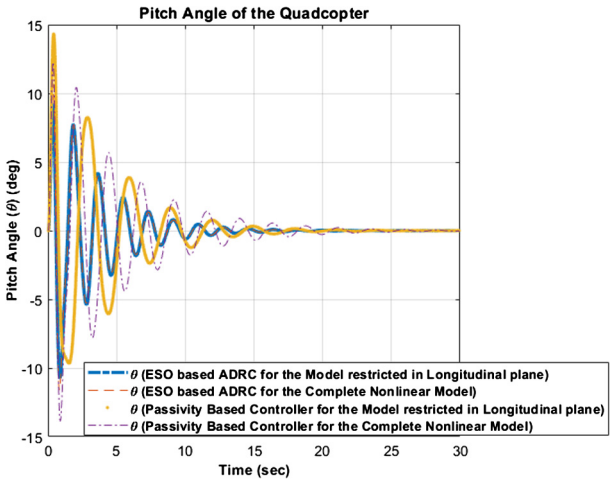

Fig. 7. Pitch angle of the quadcopter.

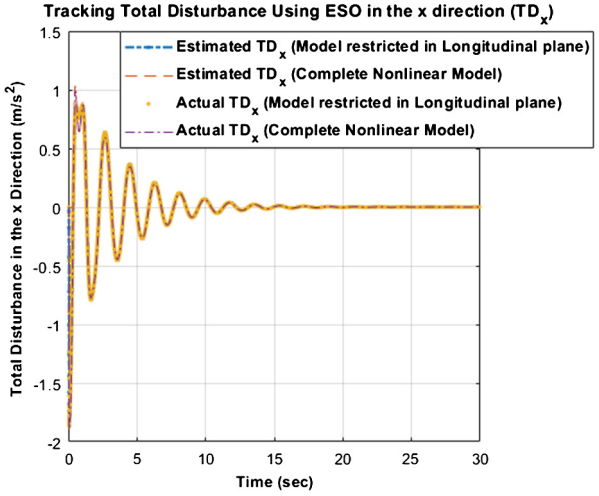

Fig. 8. Estimation of total disturbance in x direction.

are disturbances introduced in the system due to the oscillation of the payload. The controllers try to reject these disturbances while trying to maintain the altitude and the longitudinal position of the quadcopter and damping the oscillations of the payload. From Fig. 7 it can be seen that the pitch controller adjusts the pitch angle of the quadcopter thus providing necessary control to regulate the longitudinal position of the quadcopter. The pitch angle has an oscillatory behavior and it decays to zero as the payload oscillations decay and the quadcopter goes back to the initial hover pose.

The extended state observer based active disturbance rejection controller gives a better performance by damping the oscillations of the payload and controlling the altitude and the longitudinal position of the quadcopter faster than the passivity based controller when implemented on both, the mathematical model of quadcopter+payload with longitudinal plane restriction and the complete nonlinear model of quadcopter+payload. It can be seen from Fig. 8 and 9 that the extended state observer is able to track the total disturbance along the x and z direction respectively. It can be seen from Fig. 9 that the total disturbance along z direction (TD_z) converges to a value of -9.81 m/s^2 when the quadcopter goes in the hover mode, which means that when the system is stabilized, the only disturbance acting on the system is acceleration due to gravity. These estimates are used by the active disturbance rejection controller to control the position of the quadcopter and damp the oscillations of the slung payload. It can be seen from Fig. 10 that the continuous-discrete Kalman filter is also able to

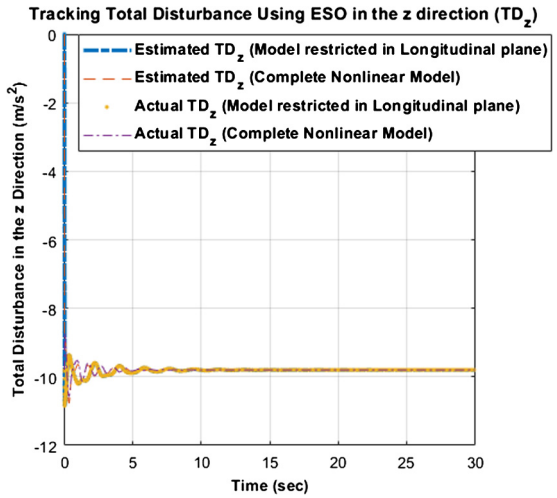

Fig. 9. Estimation of total disturbance in z direction.

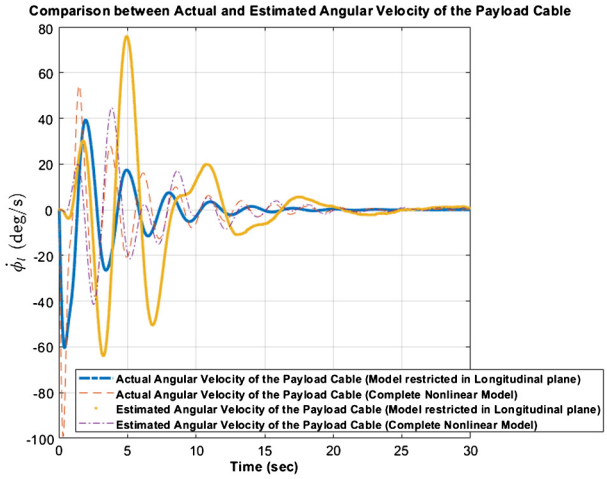

Fig. 10. Comparison between the actual and the estimated angular velocity of the payload cable using continuous-discrete Kalman filter.

track the angular velocity states of the payload cable and the passivity based controller provides a reasonable performance.

It is to be mentioned that since the payload swing motion is restricted to the longitudinal plane, the ESO based controller is more robust since the results are not any different if the implementation is on a restricted simulation or on the full nonlinear simulation. This is because, the ESO treats all of the RHS of the dynamics as an input matched disturbance. Since this is not the case in the PBC, the results vary if a restricted simulation or a full simulation are utilized.

4.2. Case 2: Quadcopter moving with a constant speed along x_i axis is commanded to go in the hover mode

At the start of the simulation, the quadcopter is in hover mode and the payload is in a stable configuration. The quadcopter is commanded to follow a straight line trajectory along x_i axis with a constant speed of 10.8 km ph (3 m/s) and fixed altitude. At 50 s, the quadcopter is commanded to go back to the hover mode. Fig. 11, 12, 13 and 14 compare the performance of the passivity based controller and the extended state observer based active disturbance rejection controller. From Fig. 11 and 12, it can be observed that the controllers are able to maintain the quadcopter altitude as well as the trajectory along x_i axis and the desired position when commanded to go back to the hover mode. From Fig. 13,

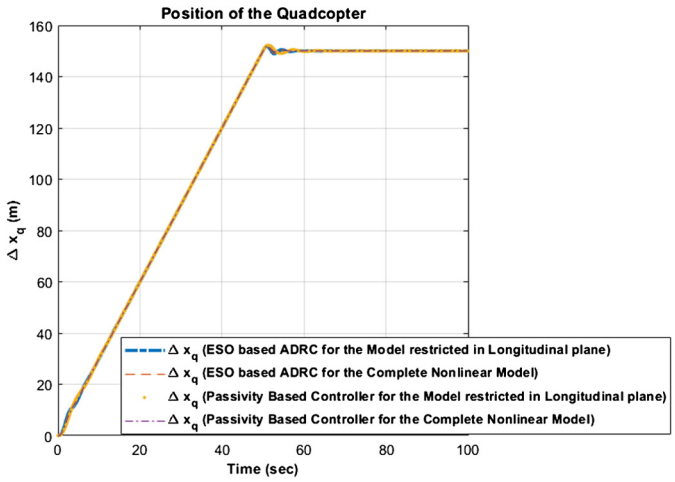

Fig. 11. Longitudinal position of the quadcopter (x_Q).

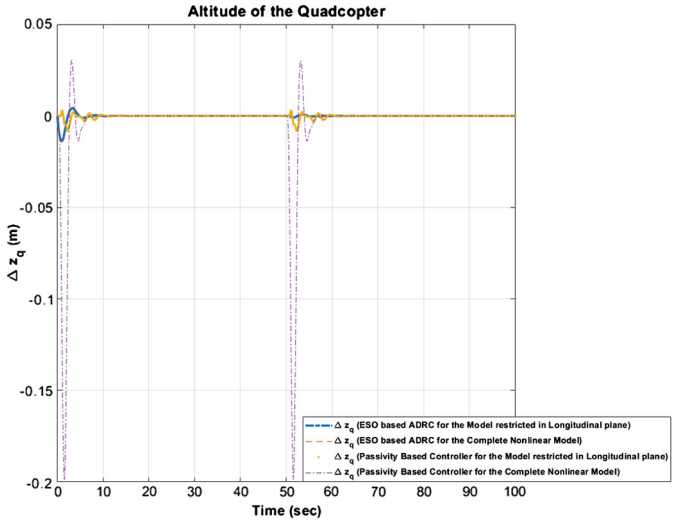

Fig. 12. Altitude of the quadcopter (z_Q).

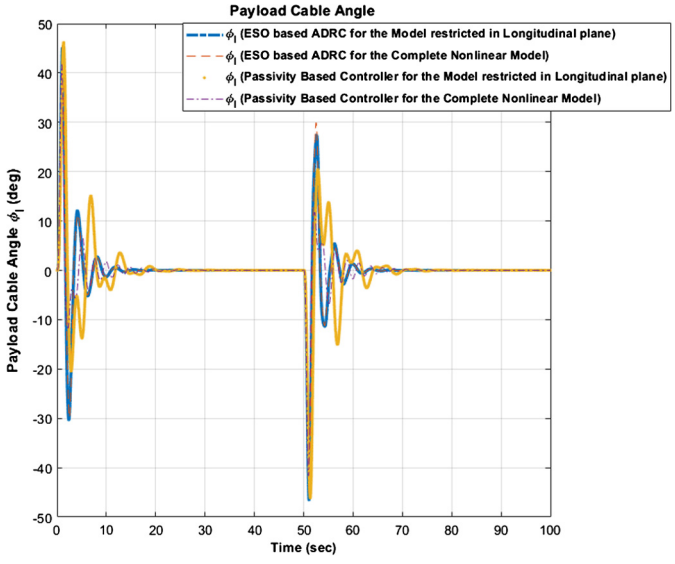

Fig. 13. Payload cable angle history.

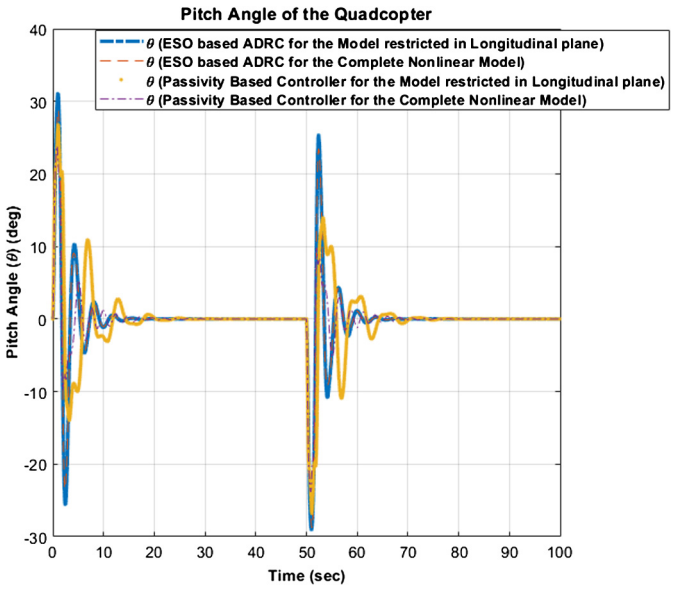

Fig. 14. Pitch angle of the quadcopter.

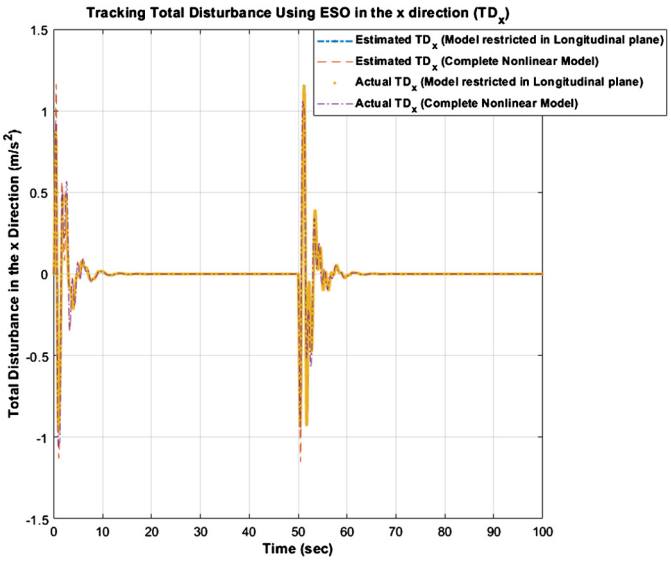

Fig. 15. Estimation of total disturbance in x direction.

it can be seen that the payload is perturbed due to changes in the quadcopter states at the start of the simulation and the controllers stabilize the payload while the quadcopter is in motion. The payload is perturbed again when the quadcopter goes back to the hover mode and the controllers are able to stabilize the system. The quadcopter position and velocity along x_i axis is maintained using the pitch angle. From Fig. 14, it is observed that the pitch angle has a decaying oscillatory behavior as the controllers try to maintain the constant speed straight line trajectory of the quadcopter while attenuating the oscillations of the slung payload due to the changes in the quadcopter states. When the quadcopter is commanded to go back to the hover mode at 50 s, the controllers try to maintain the position of the quadcopter along the x_i and attenuate the oscillations of the payload due to the changes in the quadcopter states using the pitch angle. A decaying oscillatory behavior in the pitch angle of the quadcopter is observed again as the payload oscillations decay and quadcopter goes back to the hover pose.

It can be seen that the extended state observer based active disturbance rejection controller gives a better performance by damping the oscillations of the payload and tracking the position of the quadcopter faster than the passivity based controller when implemented on both, the mathematical model of quadcopter+payload with longitudinal plane restriction and the complete nonlinear model of quadcopter+payload. It can be seen from Fig. 15 and 16 that the extended state observer is able to track the total disturbance. It can be seen from Fig. 16 that the total disturbance along z direction (TD_z) converges to a value of -9.81 m/s^2 when the translational dynamics of the quadcopter along inertial z axis (z_i) is stabilized, which means that the only disturbance acting on the system is acceleration due to gravity. These estimates are used by the active disturbance rejection controller to control the position of the quadcopter and damp the oscillations of the slung payload. It can be seen from Fig. 17 that the continuous-discrete Kalman filter overestimates the angular velocity states of the payload cable and the passivity based controller still provides a reasonable performance.

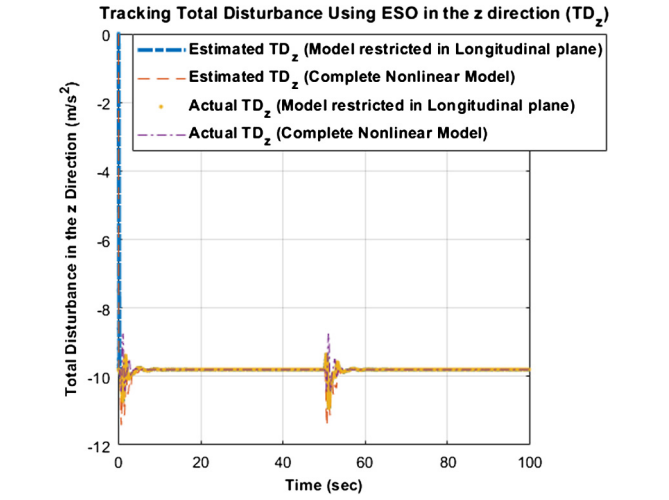

Fig. 16. Estimation of total disturbance in z direction.

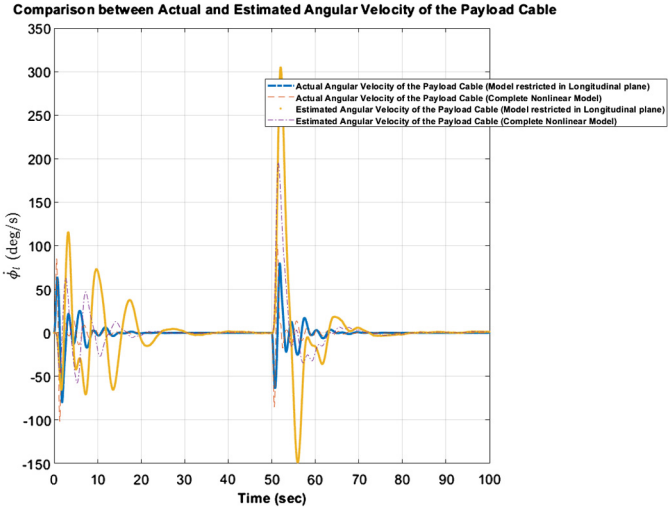

Fig. 17. Comparison between the actual and the estimated angular velocity of the payload cable using continuous-discrete Kalman filter.

5. Summary and conclusions

A comprehensive mathematical model was derived for a quadcopter with a cable suspended payload using an Euler-Lagrange formulation. A restricted degrees of freedom system (longitudinal

plane only) was then used to develop a passivity based controller and an extended state observer based active disturbance rejection controller. These were compared using a high fidelity full six degree of freedom simulation environment. The passivity based control requires that the payload swing angles and the angle rates be measured. If only the angle is measured, an estimator to synthesize the angular velocity is needed. On the other hand, the extended state observer estimates the "total disturbance" which includes the payload motion using only the quadcopter states (longitudinal position, altitude, pitch angle). The synthesis of this disturbance allows the design of a disturbance rejection controller while achieving the position tracking and regulation objectives. The tuning of the parameters for the continuous-discrete Kalman filter in case of the passivity based controller, the extended state observer, as well as the controller requires careful consideration.

Declaration of Competing Interest

No conflict of interest.

Appendix A. Parameter values used for the simulations

Table 1
Physical parameters of quadcopter and cable-slung payload.

Parameter	Value	Units
Mass of the Quadcopter, m_Q	1.2	kg
Mass of the payload, m_l	0.5	kg
Length of the Payload Cable, l	0.7	m
Inertia of the Quadcopter, I_{xx}	1.367×10^{-2}	$\mathrm{kg\,m^2}$
Inertia of the Quadcopter, I_{yy}	1.367×10^{-2}	$\mathrm{kg\,m^2}$
Inertia of the Quadcopter, I_{zz}	2.586×10^{-2}	$\mathrm{kg\,m^2}$
Arm Length of the Quadcopter, L	0.225	m

Table 2
Continuous-discrete extended Kalman filter parameters.

Parameter	Covariance	Units
Measurement Error (Zero mean White Noise Process), $v_\phi(t)$	0.01	$\mathrm{rad^2}$
Process Noise (Zero mean White Noise Process), $w_\phi(t)$	0.25	$\mathrm{rad^2/s^4}$

Table 3
Extended Kalman filter parameters.

Parameter	Value
Ω	1000
β_{z1}	3Ω
β_{z2}	$3\Omega^2$
β_{z3}	Ω^3
β_{x1}	3Ω
β_{x2}	$3\Omega^2$
β_{x3}	Ω^3

Table 4
Passivity based controller gains.

Parameter	Value
k_{pz}	5
k_{dz}	1.7
k_{px}	1
k_{dx}	0.6
$\lambda_{\boldsymbol{\Theta}}$	12
$\lambda_{\boldsymbol{\omega}}$	5

Table 5
Active disturbance rejection controller gains.

Parameter	Value
k_{pz}	2
k_{dz}	1
k_{px}	2
k_{dx}	1
$\lambda_{\boldsymbol{\Theta}}$	10
$\lambda_{\boldsymbol{\omega}}$	5

References

[1] S. Kim, S. Choi, H.J. Kim, Aerial manipulation using a quadrotor with a two DOF robotic arm, in: 2013 IEEE/RSJ International Conference on Intelligent Robots and Systems (IROS), IEEE, 2013, pp. 4990–4995.

[2] K. Sreenath, N. Michael, V. Kumar, Trajectory generation and control of a quadrotor with a cable suspended load – a differentially flat hybrid system, in: 2013 IEEE International Conference on Robotics and Automation (ICRA), IEEE, 2013, pp. 4888–4895.

[3] S. Sadr, S.A.A. Moosavian, P. Zarafshan, Dynamics modeling and control of a quadrotor with swing load, J. Robot. (2014).

[4] M.E. Guerrero-Sanchez, H. Abaunza, P. Castillo, R. Lozano, C. Garcia-Beltran, A. Rodriguez-Palacios, Passivity-based control for a micro air vehicle using unit quaternions, Appl. Sci. 7 (1) (2016) 13.

[5] M. Guerrero, D. Mercado, R. Lozano, C. García, IDA-PBC methodology for a quadrotor UAV transporting a cable-suspended payload, in: 2015 International Conference on Unmanned Aircraft Systems (ICUAS), IEEE, 2015, pp. 470–476.

[6] M.M. Nicotra, E. Garone, R. Naldi, L. Marconi, Nested saturation control of a UAV carrying a suspended load, in: Proceedings of American Control Conference, IEEE, 2014, pp. 3585–3590.

[7] M. Kanazawa, S. Nakaura, M. Sampei, Inverse optimal control problem for bilinear systems: application to the inverted pendulum with horizontal and vertical movement, in: Proceedings of the 48th IEEE Conference on Decision and Control, 2009 held jointly with the 28th Chinese Control Conference, CDC/CCC 2009, IEEE, 2009, pp. 2260–2267.

[8] I. Palunko, R. Fierro, P. Cruz, Trajectory generation for swing-free maneuvers of a quadrotor with suspended payload: a dynamic programming approach, in: 2012 IEEE International Conference on Robotics and Automation, 2012, pp. 2691–2697.

[9] S. Tang, V. Wüest, V. Kumar, Aggressive flight with suspended payloads using vision-based control, IEEE Robot. Autom. Lett. 3 (2) (2018) 1152–1159, https://doi.org/10.1109/LRA.2018.2793305.

[10] K. Sreenath, T. Lee, V. Kumar, Geometric control and differential flatness of a quadrotor UAV with a cable-suspended load, in: IEEE Control and Decision Conference, 2013.

[11] F.A. Goodarzi, D. Lee, T. Lee, Geometric control of a quadrotor UAV transporting a payload connected via flexible cable, Int. J. Control. Autom. Syst. 13 (6) (2015) 1486–1498.

[12] M. Weijers, Minimum Swing Control of a UAV with a Cable Suspended Load, Master's thesis, University of Twente, 2015, https://www.ram.ewi.utwente.nl/aigaion/publications/show/2457.

[13] H. Wang, Y. Huang, C. Xu, ADRC methodology for a quadrotor UAV transporting hanged payload, in: 2016 IEEE International Conference on Information and Automation (ICIA), 2016, pp. 1641–1646.

[14] J. Han, From PID to active disturbance rejection control, IEEE Trans. Ind. Electron. 56 (3) (2009) 900–906, https://doi.org/10.1109/TIE.2008.2011621.

[15] A. Godbole, K. Subbarao, Mathematical modeling and control of an unmanned aerial system with a cable suspended payload, in: 14th International Conference on Control and Automation (ICCA), IEEE, June 2018, pp. 12–15.

[16] R.P.K. Jain, Transportation of Cable Suspended Load Using Unmanned Aerial Vehicles: A Real-Time Model Predictive Control Approach, Master's thesis, TU Delft, Netherlands, 2015, http://resolver.tudelft.nl/uuid:4c6b4a94-4f15-4e67-8c30-eb8156aab406.

[17] J.L. Crassidis, J.L. Junkins, Optimal Estimation of Dynamic Systems, CRC Press, 2011.

[18] E. deVries, K. Subbarao, Backstepping based nested multi-loop control laws for a quadrotor, in: 11th International Conference on Control, Automation, Robotics and Vision, ICARCV 2010, 2010.